Aging Cell (2011) **10,** pp80–95 Doi: 10.1111/j.1474-9726.2010.00644.x

Somatic cell nuclear reprogramming of mouse oocytes endures beyond reproductive decline

Telma Cristina Esteves, Sebastian Thomas Balbach, Martin Johannes Pfeiffer, Marcos Jesus Araúzo-Bravo, Diana Claire Klein, Martina Sinn and Michele Boiani

Max-Planck Institute for Molecular Biomedicine, Röntgenstrasse 20, D-48149 Münster, Germany

Summary

The mammalian oocyte has the unique feature of supporting fertilization and normal development, while capable of reprogramming nuclei of somatic cells toward pluripotency, and occasionally even totipotency. While oocyte quality is known to decay with somatic aging, it is not a given that different biological functions decay concurrently. In this study, we tested whether oocyte's reprogramming ability decreases with aging. We show that oocytes isolated from mice aged beyond the usual reproductive age (climacteric) yield ooplasts that retain reprogramming capacity after somatic nuclear transfer (SCNT), giving rise to higher blastocysts rates compared to young donors ooplasts. Despite the differences in transcriptome between climacteric and young ooplasts, gene expression profiles of SCNT blastocysts were very similar. Importantly, embryonic stem cell lines with capacity to differentiate into tissues from all germ layers were derived from SCNT blastocysts obtained from climacteric ooplasts. Although apoptosis-related genes were down-regulated in climacteric ooplasts, and reprogramming by transcription factors (direct-induced pluripotency) benefits from the inhibition of p53-mediated apoptosis, reprogramming capacity of young ooplasts was not improved by blocking p53. However, more outgrowths were derived from SCNT blastocysts developed in the presence of a p53 inhibitor, indicating a beneficial effect on trophectoderm function. Results strongly suggest that oocyte-induced reprogramming outcome is determined by the availability and balance of intrinsic pro- and anti-reprogramming factors tightly regulated and even improved throughout aging, leading to the proposal that oocytes can still be a resource for somatic reprogramming when they cease to be considered safe for sexual reproduction.

Correspondence
Michele Boiani, Max-Planck Institute for Molecular Biomedicine, Röntgenstrasse 20, D-48149 Münster, Germany. Tel.: +49 251 70365 330; fax: +49 251 70365 399; e-mail: mboiani@mpi-muenster.mpg.de

Acceptance for publication *29 September 2010*

Key words: oocyte; aging; apoptosis; somatic cell nuclear transfer; reprogramming; pluripotency.

Introduction

The mammalian oocyte hosts a set of unique biological processes, such as the ability to haploidize its own DNA, to remodel sperm chromatin into a functional pronucleus, and to support preimplantation development, after which pluripotent embryonic stem cells (ESCs) can be derived. Yet another feature of the oocyte is its extraordinary ability to reprogram (i.e. to confer pluri- and totipotency on) the nuclei of somatic cells, as demonstrated by blastocyst formation or even full-term development after somatic cell nuclear transfer (SCNT). Importantly, the oocyte is also among the few cell types designed by nature to last for the animal's reproductive lifespan, implying that the cell's intrinsic qualities and functions need to be preserved extensively, over a long period of time (homeostasis).

However, the homeostatic capacity of the oocyte is reported to decay with aging, affecting sexual reproduction. Studies in the mouse show that metaphase II oocytes from older subjects are more prone to chromosome malsegregation and aneuploidy (Eichenlaub-Ritter *et al.*, 1988; Eichenlaub-Ritter, 2002), and that their transcriptome deviates from that of younger counterparts (Hamatani *et al.*, 2004; Pan *et al.*, 2008). These changes are ascribed to the deterioration of meiotic spindle integrity and of the pool of maternal transcripts, both needed for correct oocyte-to-embryo transition. Although the environment of the maternal genital tract plays an important role in developmental success (Gosden, 1974), the outcomes of age-induced altered oocyte quality are still considered to be a chief contributor to decrease in fitness for reproduction with aging (Sauer, 1998).

While processing of the sperm genome in the ooplasm is the product of an evolutionary path aimed at reproduction, somatic reprogramming is an experimental procedure developed in the past decades to test the role of genetic changes and the reversibility of epigenetic marks during cell differentiation (Beetschen & Fischer, 2004). Although fertilization is reported to be negatively affected by maternal aging (Miao *et al.*, 2009), it is not clear whether the oocyte's reprogramming capacity is preserved with aging. Even though the degradation of maternal mRNA that occurs during oocyte maturation differs dramatically between young and old mice (Pan *et al.*, 2008), and the level of degradation of maternal mRNA during the first and second cell cycle is different between fertilized and SCNT-derived embryos (Vassena *et al.*, 2007), the consequences of such discrepancies have remained uncertain or unexplored.

In this study, we aimed at determining the impact of aging-related alteration in ooplasm quality for somatic nuclear

Aging Cell

reprogramming capacity. As transcripts are left in place when the meiotic spindle is removed prior to SCNT (Balbach *et al.*, 2007), oocytes from aged and young donor mice offer a unique model system to explore how aging-induced gene expression differences affect reprogramming and the quality of the resultant SCNT embryos, without the confounding factor of oocyte-borne aneuploidy. Here, we show that ooplasts (i.e. oocytes deprived of their chromosomes) isolated from mice in reproductive decay (i.e. climacteric) reprogram somatic nuclei to a larger extent than ooplasts from young mice, as judged by preimplantation developmental rates. The two age groups present relatively small – yet significant – differences in the transcriptome, which disappear as the nucleus-transplanted ooplasts give rise to blastocysts. Importantly, ESCs could be derived from blastocysts originated from SCNT into ooplasts from climacteric mice. In light of these results, we propose that genes most relevant to nuclear reprogramming are among those most stably expressed during aging, whereas genes differentially expressed account for the observed higher nuclear reprogramming potential of climacteric oocytes. As mouse oocytes retain and even improve their reprogramming ability during reproductive decline, our results foster discussion on the use of ooplasts as useful resources for reprogramming, when intact oocytes cease to be considered safe for sexual reproduction.

Results

Female mice over 1 year old show decrease in reproductive fitness

In this study, we assessed reprogramming ability of oocytes from mice experiencing reproductive decay (climacteric) compared to oocytes from juvenile counterparts. The term 'climacteric', though more commonly applied in humans, is used throughout this manuscript to allow distinction from other studies, where the terms 'aged' and 'old' are applied not in connection to reproductive decline, but are rather used to describe situations such as *in vitro* aging or the age of donors relative to a younger group. B6C3F1 mouse oocytes were used in this study. B6C3F1 is a hybrid of inbred mouse strains with a mean lifespan of about 28 months for the female (Storer, 1966; Myers, 1978), which is comparable to the C57Bl/6 strain used in previous aging studies (Hamatani *et al.*, 2004; Huang *et al.*, 2009). In these animals, decline in reproductive fitness is already apparent at 1 year of age (Huang *et al.*, 2009); generally, decay is denoted in mice by physiological changes such as decrease in estrous cycles frequency (Nelson *et al.*, 1982) and decline in oocyte numbers (Jones & Krohn, 1961; Huang *et al.*, 2009). In our study, 50- to 62-week-old B6C3F1 mice showed signs of aging compared to 5- to 9-week-old counterparts (Fig. 1A), including a significant increase in body weight (Fig. 1A,B). In accordance with previous reports (Nelson *et al.*, 1982), evaluation of estrous cycles frequency also pointed to a decrease in the average cycle number in the older group (Fig. 1B). After PMSG priming and human chorionic gonadotropin (hCG)-induced ovulation, oocytes were collected from the oviducts of young and aged females, and ovaries were processed for histological analysis (Fig. 1C). Compared to young females, aged individuals showed a significant reduction in number of follicles per ovarian section, as well as in the number of oocytes retrieved (Fig. 1D). These observations are in agreement with previous reports using similarly aged mice (Jones & Krohn, 1961; Eppig & O'Brien, 1995; Huang *et al.*, 2009) and further confirm that the aged group used was undergoing loss of reproductive function (i.e. was climacteric).

Oocytes from young and climacteric mice have differences in oxidative stress and transcriptome

Oocytes were collected from climacteric (57–62 weeks old) and young (5–9 weeks old) superovulated B6C3F1 mice and immediately assessed for viability, ATP content, reactive oxygen species (ROS) levels, and transcriptome profile. The majority of the oocytes retrieved from oviducts of climacteric mice presented morphological characteristics of unviable germ cells, such as fragmentation, clumping of vitelline granules in the ooplasm, and increased perivitelline space. These oocytes were discarded. Only oocytes that did not exhibit these characteristics (i.e. those with lower levels of vitelline granules and normal perivitelline space) were allocated for the experiments (Fig. 1E climacteric, arrows). These oocytes were not only indistinguishable in their morphological characteristics, but also showed global ATP levels (0.43 ± 0.01 pmol per oocyte) similar to both freshly isolated (0.40 ± 0.06 pmol per oocyte) and *in vitro* aged young oocytes (0.54 ± 0.06 pmol per oocyte). Results are in agreement with a previous report showing similar ATP levels for young and postovulatory aged oocytes from B6C3F1 mice (Igarashi *et al.*, 2005), while diverging from the expected decrease in mammalian oocyte intracellular ATP concentration with natural aging (Tarín, 1996; Tarín *et al.*, 2000), which may be explained by species/strain- and age-related differences.

Despite the identified similarities in morphology and ATP levels, climacteric oocytes have higher average levels of ROS content (i.e. hydrogen peroxide and related molecules, measured by fluorescence imaging using the probe DCHFDA) compared to young counterparts (young: 0.16 ± 0.08; climacteric: 0.38 ± 0.41 arbitrary fluorescence units; Student's *t*-test, $P = 0.018$), a result that is in accordance with that previously reported (Huang *et al.*, 2009). Furthermore, global gene expression analysis revealed that ooplasts from climacteric mice have significant differences in the gene expression relative to young donors (Fig. 2A). Specifically, ooplasts were collected from the same pool used for SCNT (climacteric and young donors) and subjected to microarray analysis (Whole Mouse Genome Microarray kit; Agilent Technologies, Palo Alto, CA, USA). The obtained profiles indicate that 724 genes were differentially expressed ($\log_2$-fold change of two; Fig. 2A) between young and climacteric ooplasts (4.33% of the total

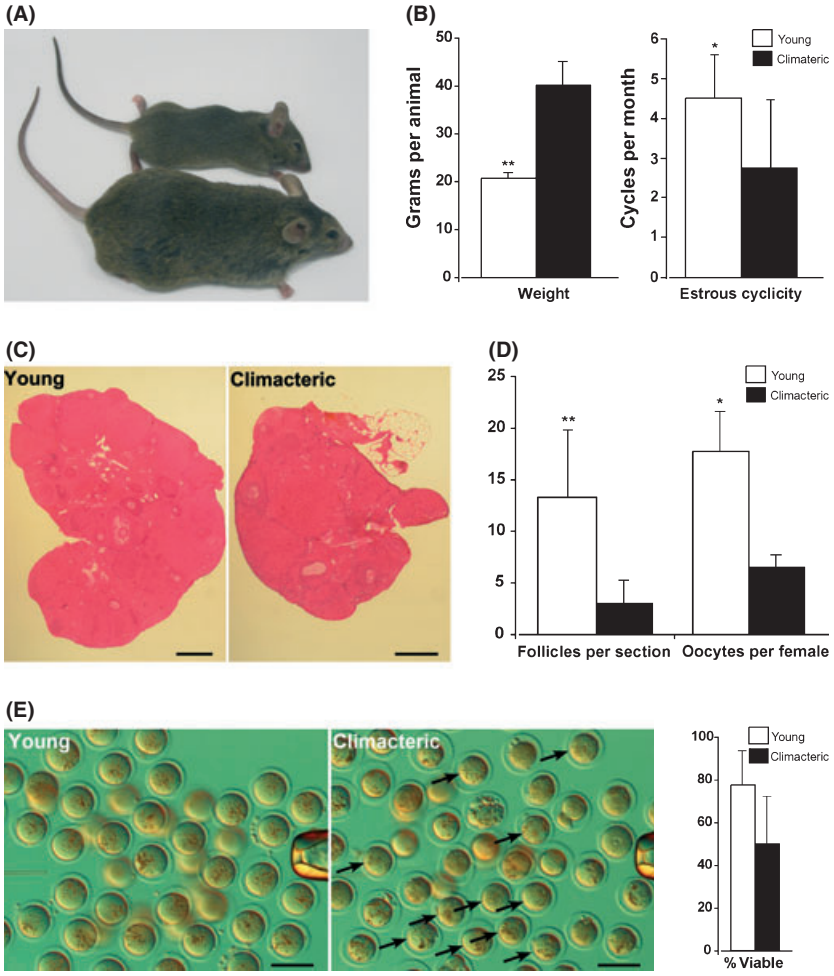

Fig. 1 Reproductive decay of 1-year-old B6C3F1 female mice. (A) Fifty-week-old B6C3F1 female (bottom mouse) shows signs of aging, like achromotrichia and hair loss, compared to 5-week-old counterpart (top mouse). (B) Further aging phenotypes include increased body weight (***t*-test, $P < 0.0005$) and lower estrous cycle frequency (**t*-test, $P < 0.05$). (C) Histological sections (eosin staining) of ovaries from young (5 weeks old) and old (57 weeks old) B6C3F1 mice; scale bar: 400 μm. (D) Average number of oocytes determined per ovarian section (***t*-test, $P < 0.0005$) and number of oocytes retrieved from oviduct after superovulation ($n = 30$ young mice, $n = 106$ climacteric mice; **t*-test, $P < 0.05$). (E) Metaphase II oocytes retrieved after superovulation of 5- (young) and 60-week-old (climacteric) B6C3F1 females. Viable oocytes were identified based on morphological evaluation (lower levels of vitelline granules and normal perivitelline space, as indicated with arrows for climacteric); scale bar: 100 μm. Percentage of viable oocytes allocated for micromanipulation is indicated.

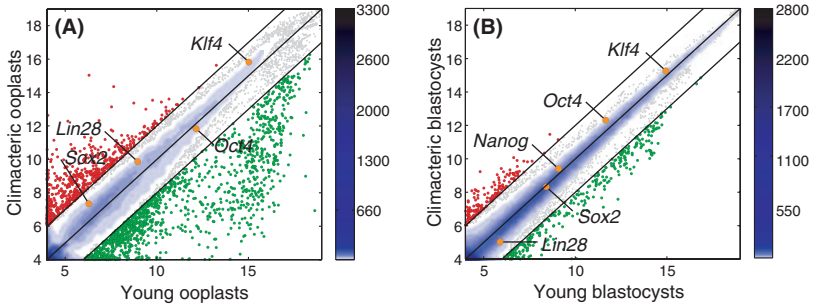

Fig. 2 Global gene expression profile of ooplasts and somatic cell nuclear transfer (SCNT)-derived mouse blastocysts. Scatter plots based on microarray data obtained for (A) ooplasts from climacteric and young mice and (B) the resultant SCNT blastocysts (climacteric blastocysts vs. young blastocysts). Black lines indicate $\log_2$-fold two changes in gene expression levels between the paired samples. Blue intensity levels indicate scattering density (the higher the scattering density, the darker the blue). The positions of some pluripotent markers (*Oct4*, *Sox2*, *Klf4*, *Lin28* and *Nanog*) are shown. Gene expression levels are scaled to $\log_2$. Green and red circles mark up- and down-regulated genes, respectively; these are used for gene ontology analysis (Table 1).

number of transcripts detected on the microarray). Gene ontology (GO) analysis for down-regulated transcripts revealed an enrichment of categories related to signal transduction, cell cycle regulation, cell growth, metabolic pathways, and apoptosis (Table 1A). Genes up-regulated in climacteric ooplasts related mainly to immune response, regulation of enzyme catalytic activity, response to stress, signaling cascades, morphogenesis, and cellular structure (Table 1B). mRNA encoding DNA-binding proteins with assigned function as transcriptional repressors were among the most highly down-regulated in climacteric ooplasts. These included the genes *Pcmt1*, *Mbd1*, *Mbd3*, *Ahrr*, *Samd11*, *Hdac1*, *Zfp263,* and *Brahma* (*Smarca2*).

Table 1 Significant gene ontology (GO) enrichment terms for differentially expressed genes between young and climacteric ooplasts. Gene ontology terms are taken from the AMIGO GO database. Significance of the GO terms of differentially expressed genes was analyzed using an enrichment approach based on the hypergeometric distribution. Significance (*P*-value) of GO terms enrichment was calculated based on the hypergeometric distribution. Process categories are listed, for genes down- (A) or up-regulated (B) in ooplasts from climacteric mice

P-value	GO: ID	GO term	Genes
(A) Genes down-regulated in climacteric ooplasts			
2.151e-003	0042596	Fear response	*Adra2a Bcl2 Grin2b Neurod2*
2.362e-003	0007264	Small GTPase-mediated signal transduction	*Arf6 Arfrp1 Cdgap Dnaja3 Dok1 Kras Lrrk1 Nras Rab12 Rab8a Rasl10a Rhobtb2 Rhou Rit2 Rock1 Rock2 Rrad Vav3*
3.560e-003	0006941	Striated muscle contraction	*Arg2 Homer1 Map2k6 Tpm1*
3.562e-003	0033077	T-cell differentiation in the thymus	*Bcl2 Dnaja3 Jmjd6 Stat5b*
4.003e-003	0008202	Steroid metabolic process	*Afp Ch25h Cyp7a1 Fdps Hsd17b6 Ldlr Lss Mbtps1 Pon1 Pxmp3 Serpina6 Stat5b*
5.494e-003	0000082	G1/S transition of mitotic cell cycle	*Bcl2 Cables1 Myb Rhou*
8.386e-003	0030029	Actin filament-based process	*Arhgef17 Bcl2 Kras Myl2 Neb Neurl2 Pdlim3 Ppp1r9a Rhou Rock1 Rock2 Wipf1*
9.583e-003	0000302	Response to reactive oxygen species	*Atp7a Bcl2 Ppp2cb Pxdn*
9.588e-003	0009612	Response to mechanical stimulus	*Gpr98 Grin2b Mkks Slc1a3*
1.238e-002	0007265	Ras protein signal transduction	*Dok1 Kras Nras Rhou Rock1 Rock2*
1.321e-002	0010035	Response to inorganic substance	*Asna1 Atp7a Nr4a2 Slc1a3*
1.427e-002	0019216	Regulation of lipid metabolic process	*Acsl4 Adipoq Pxmp3 Stat5b Vav3*
1.788e-002	0016458	Gene silencing	*Eif2c4 Mbd3 Sirt2 Tnrc6a Tnrc6b*
1.826e-002	0043523	Regulation of neuron apoptosis	*Akt1s1 Atp7a Bcl2 Kras Nr4a2 Rock1*
1.902e-002	0042445	Hormone metabolic process	*Ace Afp Aldh1a3 Ece2 Foxa1 Serpina6 Stat5b*
2.709e-002	0008629	Induction of apoptosis by intracellular signals	*Bcl3 Casp3 Diablo Eaf2*
2.819e-002	0043066	Negative regulation of apoptosis	*Akt1s1 Bag3 Bcl2 Bcl3 Casp3 Cx3cl1 Kras Nr4a2 Ppp2cb Prnp Prop1 Rock1 Rrn3 Stat5b*
3.514e-002	0006457	Protein folding	*Cct3 Dnaja1 Dnaja3 Fkbp11 Fkbp2 Fkbp4 Pin1 Ppie Slmap*
3.594e-002	0045664	Regulation of neuron differentiation	*Bcl2 Foxa1 Isl1 Mib1 Plxnb2 Prpf19 Sema3a*
3.831e-002	0033500	Carbohydrate homeostasis	*Adipoq Foxa1 Pdx1 Ptch1*
3.835e-002	0046700	Heterocycle catabolic process	*Afmid Amdhd1 Entpd2 Phf11*
3.863e-002	0051604	Protein maturation	*Adamts3 Aga C2 Cd55 Ece2 Prss12 Ptch1*
4.095e-002	0001558	Regulation of cell growth	*Bcl2 Crim1 Eaf2 Igfbp6 Sertad2*
4.257e-002	0009064	Glutamine family amino acid metabolic process	*Aldh4a1 Amdhd1 Arg2 Slc1a3*
4.455e-002	0060562	Epithelial tube morphogenesis	*Bcl2 Dag1 Npnt Ptch1 Src*
(B) Genes up-regulated in climacteric ooplasts			
3.929e-005	0002712	Regulation of B-cell-mediated immunity	*Fcer1g Fcgr1 Ptprc Stat6 Tnfsf13*
2.709e-004	0009611	Response to wounding	*Atrn Ccl5 Clec7a Fcgr1 Fntb Lcp1 Nf1 Orm1 Pecam1 Saa4 Tnfrsf1b*
2.511e-003	0030799	Regulation of cyclic nucleotide metabolic process	*Adcy7 Gnas Gucy1a3 Nf1 Timp2*
3.438e-003	0006950	Response to stress	*A730011L01Rik Apaf1 Atrn C1qc Ccl5 Clec7a Fcer1g Fcgr1 Fntb Hspb3 Lcp1 Lig3 Map2k7 Mapk10 Nf1 Orm1 Pecam1 Polr3e Prdx6 Ptprc Rbm3 Saa4 Shprh Smpd3 Srxn1 Tnfrsf1b Xrcc2*
4.949e-003	0000165	MAPKKK cascade	*Map2k7 Mapk10 Nf1 Shank3*
2.032e-002	0043085	Positive regulation of catalytic activity	*Adcy7 Apaf1 Dgkq Gadd45g Gnas Nf1 Ptprc Tgm2*
2.131e-002	0007420	Brain development	*Apaf1 Myh10 Nf1 Sept4*
3.095e-002	0030036	Actin cytoskeleton organization	*Aif1 Capn3 Lcp1 Myh10 Nckap1 Nf1*
3.103e-002	0002521	Leukocyte differentiation	*Cd8a Chuk Gadd45g Lilrb3 Ptprc*
3.645e-002	0048646	Anatomical structure formation involved in morphogenesis	*Acvrl1 Apaf1 Cacna1s Capn3 Kdr Myh10 Nckap1 Shank3 Tgm2*
3.753e-002	0051128	Regulation of cellular component organization	*Bin1 Clasp1 Clec7a Col5a1 Fcer1g Fcgr1 Gna12 Myh10 Wnt7a*

Furthermore, transcriptome results were compared to those previously obtained for whole oocytes from aged C57Bl/6 donor mice (Hamatani *et al.*, 2004). Based on GO analysis, both studies share high similarity regarding the effects of aging on oocyte gene expression (e.g. down-regulation of apoptosis-related genes with aging), while some discrepancies were found for specific genes (Fig. S1, Supporting Information). mRNA levels for selected genes of interest in the ooplast were further confirmed by quantitative RT–PCR, and results were similar to those found by microarray (Fig. S2, Supporting Information).

Climacteric mouse oocytes support somatic cell nuclear reprogramming to blastocyst

Given the above-mentioned differences in global gene expression, we aimed at determining whether climacteric oocytes have altered potential for somatic nuclear reprogramming. Oocytes

Table 2 Development rates to blastocyst obtained from young and climacteric oocytes after somatic cell nuclear transfer (SCNT) and ICSI

Oocyte donor (weeks)	SCNT				ICSI		
	Oocytes	1-Cell	4-Cell (%)	Blastocyst (%)	Oocytes	1-Cell	Blastocyst (%)
5–9	240	175	128 (73.7)	53 (30.2)	219	155	102 (65.8)
57–62	178	129	77 (59.7)	57 (44.2)	114	84	68 (80.9)
Fisher's exact test†	n.a.	n.d.	$P = 0.018$	$P = 0.0157$	n.a.	n.d.	$P = 0.0165$

Two independent experiments were performed for ICSI and SCNT. Oocytes indicate the number of oocytes that were micromanipulated for enucleation; from these, oocytes were allocated to SCNT and other experiments. One-cell indicates the number of oocytes that survived micromanipulation (enucleation and SCNT). Percentages are based on the number of embryos reaching the relevant stage, from the number of the micro-manipulated oocytes (one-cell).
n.a., not applicable; n.d., not determined.
†Comparison relative to the one-cell stage; two-tailed test.

ovulated from climacteric and young mice were enucleated (i.e. were deprived from their chromosomes) and used as recipients for SCNT of cumulus cell nuclei from a young donor. Results show that the rate of blastocyst formation was higher for climacteric oocytes compared to the young group (Table 2, Fisher's exact test, $P = 0.016$). Also, while SCNT embryos from climacteric oocytes suffered higher developmental attrition until the four-cell stage compared to young counterparts processed in parallel (Table 2, Fisher's exact test, $P = 0.018$), development from four-cell to blastocyst occurred at higher rates for SCNT embryos derived from climacteric oocytes (Fisher's exact test, $P = 6.277 \times 10^{-6}$). Likewise, the developmental rate to blastocyst of the control ICSI embryos was higher for climacteric than for young donor's oocytes (Table 2, Fisher's exact test, $P = 0.016$). ATP content was also determined, revealing similar levels for ICSI blastocysts derived from young (0.19 ± 0.04 pmol per embryo) and climacteric (0.20 ± 0.04 pmol per embryo) oocytes. Moreover, ICSI blastocysts from both age groups showed indistinguishable levels of hydrogen peroxide and related molecules (measured by fluorescence imaging; Student's *t* test, $P = 0.876$), further indicating similarity in basic metabolic and oxidative parameters at the end of pre-implantation development.

Age-associated changes in ooplast gene expression leave marks on embryonic stages

Given the observed differences in transcriptome composition and blastocyst formation of young and climacteric oocytes, we further examined the quality of reprogramming, i.e. beyond the level of information given by developmental rates. To this end, cumulus cells from one 8-week-old mouse donor expressing an Oct4 promoter-driven green florescent protein (GFP) transgene were used for nuclear transplantation into young and climacteric ooplasts. In a previous report, we demonstrated that GFP intensity levels of embryos derived from transfer of somatic Oct4-GFP nuclei correlate positively not only with blastocyst rate, but also with levels of endogenous pluripotency markers, ESCs derivation success, and probability of fetal formation after embryo transfer (Cavaleri *et al.*, 2008). Live-cell quantitative imaging of SCNT embryos at the morula stage (Fig. 3A) showed that GFP intensity correlated positively with blastocyst formation, for both

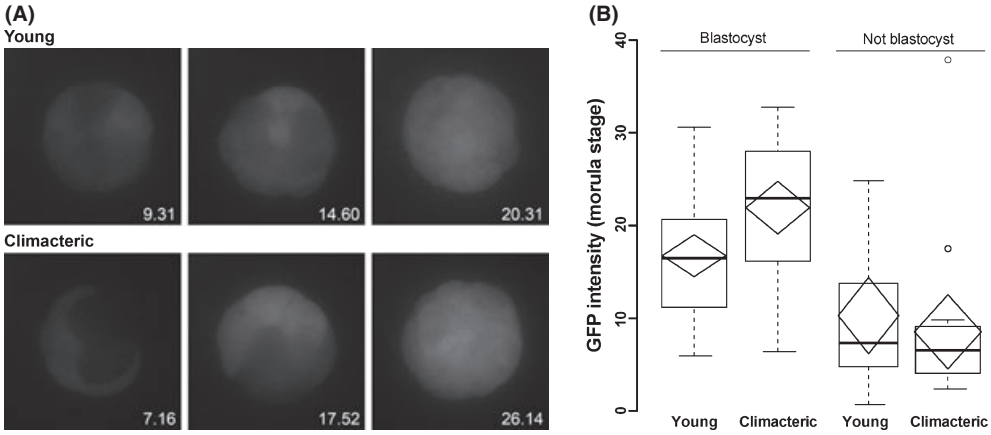

Fig. 3 GFP intensity levels in somatic cell nuclear transfer (SCNT) embryos derived from young and climacteric oocytes. Nuclei from Oct4-GFP transgenic cumulus cells were used for SCNT into young and climacteric ooplasts. (A) GFP intensities of whole embryos were measured 72-h postactivation (morula stage). Inserts indicate intensity values (gray values in arbitrary fluorescence units) of each morula shown, after background subtraction. (B) Distribution of fluorescence intensities at the morula stage, stratified by blastocyst formation (embryos derived from young and climacteric oocytes). In box plot, top and bottom lines indicate inter-quartile range, middle line indicates median, and whiskers indicate range of variation limited to 1.5 times inter-quartile range. The diamond plot represents mean and confidence intervals.

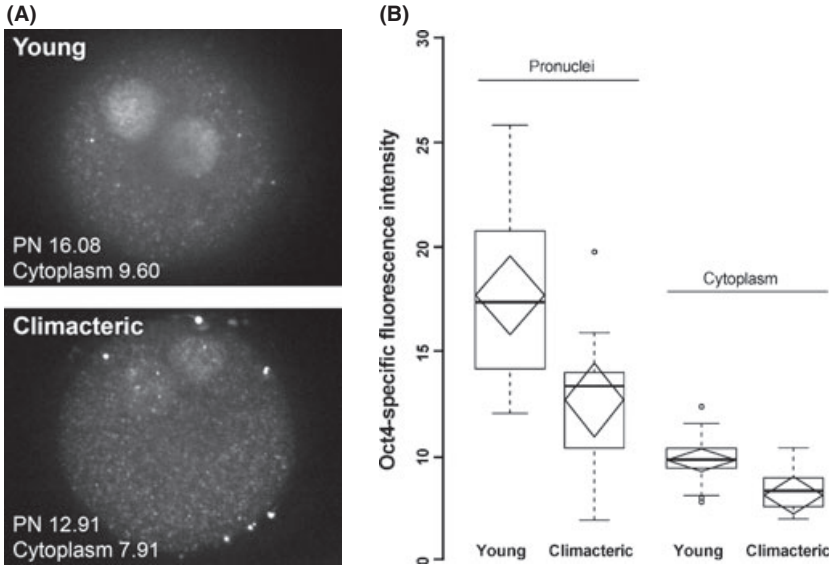

Fig. 4 Oct4 immunostaining in young and climacteric oocytes. Oocytes retrieved from young and climacteric mice were activated to pronuclear stage and processed for Oct4 detection (immunofluorescence). (A) Oct4-specific signal intensity of pronuclei (PN) and cytoplasm were measured separately, in the confocal sections containing the largest area of each pronucleus; inserts indicate average intensity values – gray values in arbitrary fluorescence units – in each oocyte shown, after background subtraction. (B) Distribution of fluorescence intensities of PN and cytoplasm, for young and climacteric oocytes. In box plot, top and bottom lines indicate inter-quartile range, middle line indicates median, and whiskers indicate range of variation limited to 1.5 times inter-quartile range. The diamond plot represents mean and confidence intervals.

age groups (fit to logistic regression model, $P = 0.00036$). Importantly, GFP intensities were generally higher for embryos derived from climacteric ooplasts, particularly among the embryos that successfully achieved the blastocyst stage (Fig. 3B). As Oct4 can bind and activate its own promoter (Boyer *et al.*, 2006), the higher Oct4-GFP signal in the morula could stem from higher oocytic content of Oct4. Immunostaining (Fig. 4A) showed that climacteric oocytes contain lower levels of Oct4 than young counterparts (Fig. 4B) in the pronuclei (Wilcoxon rank sum test, $P = 0.0020$) and cytoplasm (Welch Two Sample *t*-test, $P = 0.0007$), suggesting that the higher efficiency of climacteric oocytes after SCNT (measured as blastocyst formation and Oct4-GFP expression) is not dependent on maternal levels of Oct4.

To further assess the impact of the initial differences between climacteric and young ooplasts, transcriptome analysis was performed at the blastocyst stage (hierarchical clustering of all samples shown in Fig. S3, Supporting Information). Results showed higher level of similarity (98.7%, $R = 0.983$), compared to that observed between climacteric and young ooplasts (95.7%, $R = 0.917$; Fig. 2B). Gene ontology analysis of genes differentially expressed in SCNT blastocysts (Table S1, Supporting Information) shows preservation of differences with aging already detected at the ooplast level. These include enrichment of identities associated with hormone metabolism (down-regulation with aging), as well as enzyme catalytic activity and regulation of cellular compartment organization (up-regulation). Other enriched categories showed differential regulation in ooplasts and blastocysts with reproductive decline, such as regulation of the MAP kinase cascade (up in ooplasts, down in SCNT blastocysts) and small GTPases (down in ooplasts, up in SCNT blastocysts). Interestingly, in SCNT blastocysts, significant GO enrichment of terms down-regulated with reproductive decline are mainly related to processes occurring at the level of the plasma membrane and interface with the extracellular space. Overall, results show some level of preservation of the transcriptome differences with aging after somatic nuclear reprogramming by the ooplast, but also indicate changes in gene expression that suggest impaired interaction with the environment, for SCNT blastocysts derived from climacteric ooplasts.

Blastocysts derived from SCNT using climacteric ooplasts yield pluripotent ESCs

We further tested whether blastocysts derived from SCNT into climacteric ooplasts could give rise to pluripotent ESCs, with full differentiation capacity. Climacteric SCNT blastocysts cultured on feeder cells showed efficient outgrowth formation, at rates similar to those obtained with young SCNT blastocysts under the same experimental conditions (Table 3). Four ESC lines were

Table 3 Development rates to blastocyst and outgrowth formation obtained from young and climacteric oocytes after somatic cell nuclear transfer (SCNT)

Oocyte donor (weeks)	Oocytes	1-Cell	Blastocyst (%)	Plated	Outgrowth (%)
5	206	183	68 (37.2)	68	49 (72.1)
47–56	190	129	69 (53.5)	69	50 (72.5)
Fisher's exact test*	n.a.	n.d.	$P = 0.0054$	n.a.	$P = 0.0165$

Results are from one experiment using young oocytes and one experiment using climacteric oocytes (cumulus cell nuclei for SCNT originated from OG2 mice of the same brood). Oocytes indicate the number of oocytes that were micromanipulated for enucleation; one-cell indicates the number of oocytes that survived micromanipulation (enucleation and SCNT). Percentages are relative to the number of one-cell for blastocyst rates and to the number of blastocysts for outgrowth rates. Plated refer to blastocysts used for outgrowth formation (culture on mouse embryonic fibroblasts).

n.a., not applicable; n.d., not determined.

*Comparison relative to the one-cell stage for blastocyst rates and blastocyst plated for outgrowth rates; two-tailed test.

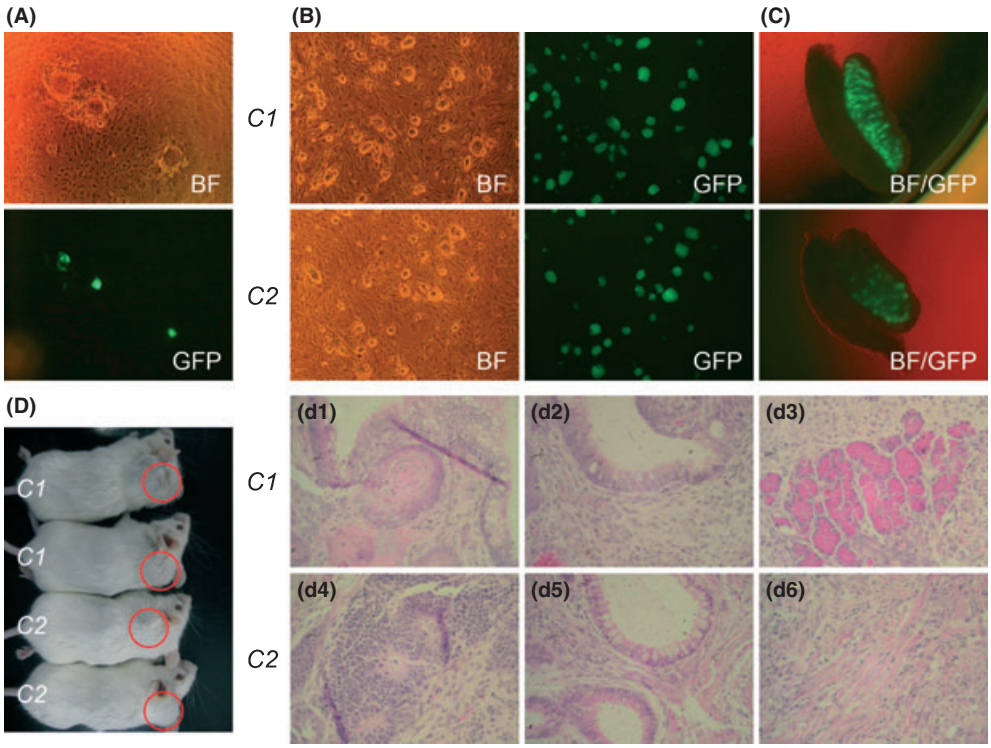

Fig. 5 Derivation and characterization of embryonic stem cells (ESCs) derived from somatic cell nuclear transfer (SCNT) into climacteric ooplasts. (A) Outgrowth of blastocysts derived from SCNT of cumulus cell nuclei transgenic for Oct4-GFP into climacteric ooplasts, cultured onto mouse embryonic fibroblast feeders. (B) Two ESC lines – *C1* and *C2* – were derived. (C) ESCs injected into fertilized blastocysts contributed to the germline of 15 dpc embryos. (D) ESCs injected subcutaneously in the neck region of SCID mice gave rise to teratomas (indicated by red circle). Histological sections (hematoxylin and eosin staining) of teratomas show tissues from all three germlayers (line *C1*, d1–d3; line *C2*, d4–d6). d1, keratinized squamous cell epithelium (ectoderm); d2, intestinal (mucosa lined) cavity (endoderm); d3, striated muscle (mesoderm); d4, neuronal rosettes (ectoderm); d5, intestinal (mucosa lined) cavity (endoderm); and d6, smooth muscle (mesoderm).

derived from climacteric SCNT blastocysts, of which two lines were tested (Fig. 5B). Upon injection into fertilized blastocysts at passage 15, both cell lines showed contribution to the germline (Fig. 5C). The capacity of these ESCs to differentiate into the three germ layers (ectoderm, mesoderm, endoderm) was assessed by differentiation protocols *in vitro*, as well as *in vivo* (by the teratoma assay). Both ESC lines could be differentiated into tissues representative of the germ layers, *in vivo* (Fig. 5D) and *in vitro* (Fig. S4, Supporting Information). These results demonstrate full pluripotentiality of the climacteric-derived SCNT-ESCs, establishing that oocytes retrieved at reproductive decline are reliable resources for somatic reprogramming.

Role of the p53 pathway in oocyte-induced reprogramming after SCNT

Based on the GO analysis results, we assessed the extent to which oocytic factors showing disturbed regulation during aging may account for the observed increased reprogramming potential of climacteric ooplasts. In this context, among the significant differences between young and climacteric oocytes, apoptosis-related pathways are candidate targets for investigation. As shown (Table 1), apoptosis signaling pathways are affected in climacteric ooplasts, including down-regulation of apoptotic intracellular signaling and response pathways, as well as up-regulation of factors with noncanonical anti-apoptotic function, such as Dnmt1 (Brown & Robertson, 2007). Importantly, recent reports showed that the inhibition of apoptosis increases the efficiency of somatic nuclear reprogramming using direct induced pluripotency (iPS) technology (Banito *et al.*, 2009; Kawamura *et al.*, 2009; Marión *et al.*, 2009). In this context, we tested whether inhibition of p53-induced apoptosis signaling also allows enhancement of reprogramming capacity by the oocyte. To this end, we cultured SCNT and ICSI embryos derived from ooplasts of young donors in the presence of pifithrin-α, a p53-specific inhibitor (Jin *et al.*, 2009). We observed a small but significant increase in rates of blastocyst formation for ICSI embryos, but no significant change on SCNT blastocyst rates (Fig. 6A). Somatic cell nuclear transfer and ICSI were also performed using cumulus cell nuclei and sperm from donors carrying the Oct4-GFP transgene and the resultant embryos cultured in the presence of pifithrin-α. Imaging of the morulae showed a small increase in GFP levels upon inhibition of p53 in both SCNT and ICSI (Fig. 6B), albeit lack of statistical significance. Interestingly, SCNT embryos treated with 1 μM pifithrin-α gave rise to a larger percentage of outgrowths compared to the untreated group; increase in outgrowths numbers with pifithrin-α treatment was less prominent for ICSI.

(A)

	SCNT				ICSI			
Pifithrin (μM)	1-cell	Blastocyst (%)	Blastocysts plated	Outgrowth (%)	1-cell	Blastocyst (%)	Blastocysts plated	Outgrowth (%)
0	64	21 (32.8)	15	8 (53.3)	47	32 (68.1)	32	23 (71.9)
1	71	24 (33.8)	16	13 (81.3)	45	39* (86.7)	39	29 (74.4)
5	71	25 (35.2)	15	9 (60.0)	45	32 (71.1)	32	20 (62.5)

Results are from two combined SCNT and one ICSI experiments (performed in parallel with one SCNT experiment).
Percentages are relative to the number of micromanipulated oocytes (1-cell), for blastocyst rates, and relative to the number of blastocysts, for outgrowth rates.
Blastocysts plated refer to embryos used for outgrowth formation (culture on MEFs).
*: p=0.047 (Fisher's exact test), for comparison relative to experiment in the absence of pifithrin (control); 2-tailed test.

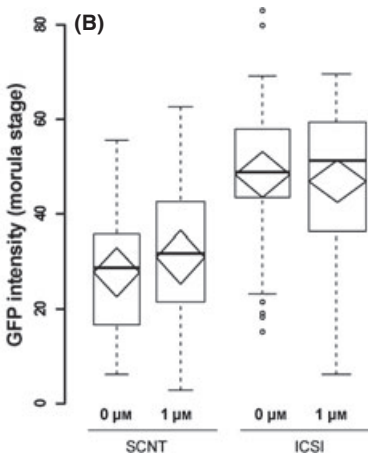

Fig. 6 Developmental rates and GFP intensity levels for somatic cell nuclear transfer (SCNT) and ICSI embryos, in the presence of p53-inhibitor pifithrin-α. (A) Blastocyst and outgrowth formation rates for embryos cultured in the absence of presence of pifithrin-α. (B) Distribution of GFP fluorescence intensities of morulae derived from SCNT or ICSI using cumulus nuclei or sperm (respectively) from OG2 mice, cultured in the absence or presence of 1 μM pifithrin-α. In box plot, top and bottom lines indicate inter-quartile range, middle line indicates median, and whiskers indicate range of variation limited to 1.5 times inter-quartile range; diamond plot represents mean and confidence intervals.

Discussion

Oocyte aging and the regulation of somatic nuclear reprogramming to pluripotency

Global decay of biological functions is a trademark of aging, with oxidative damage, membrane degradation, mitochondrial function decline, and irreparable damage accumulation as leading causes of senescence (Johnson *et al.*, 1999; Yu & Chung, 2006). Ultimately, DNA damage and chromosome instability are regarded as a main cause for reproductive decline with aging, as mutations accumulate in the germline, which can affect DNA replication, repair, and chromosome segregation (Woodruff & Thompson, 2003). Furthermore, maternal age shows positive correlation with aneuploidy rate, in human (Pellestor *et al.*, 2004) as well as in laboratory mouse strains (Eichenlaub-Ritter *et al.*, 1988; Pan *et al.*, 2008). However, whether reproductive senescence affects the ability of the oocyte to reprogram somatic nuclei has not yet been addressed. While reproductive success relies on the correct chromosomal makeup of the female gamete, oocyte-induced reprogramming function is independent of intrinsic meiotic chromosome integrity, as the metaphase II chromosomal spindle is removed prior to SCNT. However, as follicle atresia affects ooplast quality (Wang & Sun, 2007) and as there is recruitment of atretic follicles during reproductive decline in the mouse (Gosden *et al.*, 1983), the adequacy of oocytes for reprogramming with aging is put into question. Moreover, the observation that mouse oocytes retrieved after superovulation, which also recruits oocytes from atretic follicles (Peters *et al.*, 1975), are less apt to support development after SCNT compared to naturally ovulated counterparts (Hiiragi & Solter, 2005) further suggests that oocyte-mediated reprogramming will be negatively affected by aging.

In this study, we demonstrate that oocytes retrieved from mice in reproductive decline not only retain the ability to support somatic nuclear reprogramming to pluripotency after SCNT, but even possess higher reprogramming capacity compared to young counterparts, as shown by the significant increase in blastocyst rates and higher levels of the pluripotency marker Oct4-GFP. Somatic cell nuclear transfer blastocysts derived from climacteric oocytes formed outgrowths that supported the derivation of ESCs with full pluripotency, as measured by differentiation *in vitro* and *in vivo* and germline contribution. These results suggest that the decisive factors determining reprogramming are tightly regulated during reproductive decline with aging, which is consistent with the detection of normal transcript levels of endogenous pluripotency-associated factors in climacteric ooplasts. In turn, genes found differentially expressed are suggested to potentially encode factors that determine the observed improvement of reprogramming and developmental potential to blastocyst. Compared to the distinct gene expression profiles of climacteric and young oocytes, the transcriptomes of derivative SCNT blastocysts are almost indistinguishable from each other. This suggests that, while accounting for differences in reprogramming capacity (for example, by facilitation of chromatin remodeling), differences in ooplast transcriptome during reproductive decay have low impact on gene expression pattern of the preimplantation SCNT embryo itself. However, while of small magnitude, the gene expression differences between SCNT blastocysts may concern genes that are important for blastocyst viability, such as those regulating processes occurring at the level of the plasma membrane and interface with the extracellular space. Together, results strongly indicate a combination of tight homeostatic regulation of pluripotency and intrinsically determined embryo selection mechanisms with aging.

Oocyte-mediated reprogramming: natural vs. *in vitro* aging

The impact of ooplast quality decay on pluripotency induction and maintenance has been evaluated previously in various mammalian models. In the mouse, SCNT has been previously performed using oocytes lacking the second polar body and pronucleus after *in vitro* insemination (fertilization-failure oocytes), based on time in culture without signs of fertilization (Wakayama *et al.*, 2007) or based on delayed collection from the oviduct after superovulation (Taniguchi *et al.*, 1996; Liu *et al.*, 2007). In these studies, SCNT blastocyst rates were significantly lower compared to those after SCNT using freshly retrieved oocytes. Also in human, SCNT using oocytes aged *in vitro* resulted in poor developmental outcomes, which were attributed to abnormalities reflected in aberrant spindles and altered transcription profiles (Hall *et al.*, 2007). Reasons for the decrease in blastocyst rates compared to the present study may include discrepancies in micromanipulation procedure, culture conditions, and mouse strain- or species-specific differences, but also higher biological degradation of the oocytes. In this context, it is possible that *in vitro* aging or alterations linked to fertilization failure have a global negative effect on the pluripotency maintenance network, making such oocytes less suitable sources for somatic nuclear reprogramming compared to cells of aged donors.

Improving reprogramming efficiency through changes in ooplast quality

In the present study, ooplasts of climacteric mice are suggested to contain cytoplasmic factors, or altered levels thereof, that carry advantages for the preimplantation events following SCNT. Ono and colleagues showed that inhibition of class IIb histone deacetylases (Hdac6, Hdac10) in mouse oocytes of young donors resulted in a marked increase in blastocyst rates after SCNT (Ono *et al.*, 2010). With these results, Ono and colleagues suggest that weakening certain activities in the oocyte (such as that of the mentioned histone deacetylases) benefits reprogramming. Notably, in our study, mRNA for DNA-binding proteins with assigned function as transcription repressors were among the most down-regulated in climacteric ooplasts. Such chromatin modifiers could impair reprogramming efficiency after SCNT by untimely triggering transcriptional repression in the somatic nucleus (Surani, 2001; Shi *et al.*, 2003), a hypothesis also substantiated by the improvement in developmental success of mouse SCNT embryos in presence of an inhibitor of histone deacetylase trichostatin A (Kishigami *et al.*, 2006), as well as increase in iPS efficiency upon inhibition of chromatin-silencing modulators (Huangfu *et al.*, 2008; Shi *et al.*, 2008). Therefore, it is possible that what has been altered by chemical means in the experimental setting of Ono and colleagues has been at least in part achieved during natural aging. In this context, the climacteric mouse is suggested to be a suitable model to explore the nature of the effectors involved in oocyte-induced reprogramming.

Ooplast quality and pluripotency maintenance

As implied in the above discussion, effectors in place during and after oocyte-induced reprogramming are expected to relate, to a large extent, to the putative reprogramming factors conferring pluripotency on ESC-somatic cell fusion hybrids and iPS cells. Results presented here indicate that while mRNAs encoding certain pluripotency-associated transcription factors, such as *Fubp3*, *Zfp42* and *Spic* (Kim *et al.*, 2008), were down-regulated with aging, mRNAs of prominent genes linked to reprogramming and pluripotency (such as *Sox2*, *Klf4* and *Lin28*) were found to be among those showing no change between young and climacteric ooplasts. Interestingly, while no difference was detected in *Oct4* mRNA content between oocytes from young and climacteric donors, Oct4 protein was significantly more abundant in young oocytes. This agrees with the observation that *Oct4* mRNA is detected in both ooplasts and blastocysts at the same levels, whereas protein levels build up during early cleavages (Palmieri *et al.*, 1994). As young oocytes show decreased reprogramming capacity compared to climacteric oocytes, our results strengthen the hypothesis that aging positively influences reprogramming capacity by specifically altering factors whose activity repress the oocyte's reprogramming machinery. In parallel, as the detection of Oct4 in single oocytes – only now possible because of improved imaging techniques and immunocytochemistry protocols – shows different levels for oocytes with different reprogramming potential, we suggest that either maternal Oct4 is not directly involved in oocyte-mediated reprogramming efficiency, or that other factors play a more prominent role. In summary, our data reinforce the complexity of the network required for oocyte-induced reprogramming and pluripotency maintenance, which must occur at both the transcriptional and translational level, involving multiple factors.

Apoptosis and oocyte-induced reprogramming

Microarray data presented here show significant changes in ooplast global gene expression during decline in reproductive fitness. This finding is in line with the reports on oocytes of other mouse strains (Hamatani *et al.*, 2004; Pan *et al.*, 2008), and also single human oocytes (Grøndahl *et al.*, 2010). Among the detected changes, ooplasts from climacteric mouse donors expressed lower levels of mRNAs related to apoptosis (induction and negative response), compared to young counterparts. While programmed cell death prior to blastocyst formation in human has been suggested to be linked to embryo arrest (Jurisicova *et al.*, 1996), early apoptotic events are reported to play a distinct role during oocyte development, and in particular to be indicative of improved developmental potential, as shown for bovine oocytes (Li *et al.*, 2009). Also, genetic ablation of the pro-apoptotic protein Bax leads to an enhancement of oocyte survival in aged mice (Kujjo *et al.*, 2010), as well as to the minimization of age-associated problems in old females, including an extension of fertile potential (Perez *et al.*, 2007). In our study, SCNT embryos derived from climacteric ooplasts experienced

higher preimplantation developmental arrest before the four-cell stage, i.e. earlier attrition stage compared to embryos derived from young ooplasts. This observation suggests that in a situation of stress, induced for example during micromanipulation, anti-apoptotic responses at the protein level may not yet be in place in climacteric ooplasts, leading to early SCNT embryo arrest until the relevant mRNAs are translated. Furthermore, while more SCNT embryos derived from climacteric oocytes accomplish preimplantation (as shown by higher blastocyst rates) compared to young SCNT embryos, both groups have similar capacity to form outgrowths. As outgrowth formation is an *in vitro* model for implantation of the blastocyst in the uterus, this result anticipates that the rates of implantation and postimplantation development are similar between young and climacteric-derived SCNT embryos, suggesting that the initial developmental advantage of climacteric SCNT embryos is limited to preimplantation.

Recently, a link between apoptotic signaling and somatic cell reprogramming has been established. Specifically, iPS reprogramming is blocked upon induction of DNA damage response and p53-dependent apoptosis (Marión *et al.*, 2009). Furthermore, the efficiency of reprogramming somatic cells is substantially increased by ablating senescence inducers (Banito *et al.*, 2009), reducing signaling to p53 or directly silencing p53 itself (Kawamura *et al.*, 2009). Our results indicate that genes associated with negative regulation of apoptotic signaling are downregulated in climacteric ooplasts (i.e. precisely those ooplasts showing improved reprogramming capacity). We therefore investigated whether blocking the p53-mediated apoptosis pathway would have beneficial effects on oocyte-mediated reprogramming and pluripotency by young oocytes. Interestingly, the presence of the p53 inhibitor pifithrin-α during *in vitro* culture led to an increase in rates for ICSI blastocyst, but only to a small extent for SCNT embryos. A previous study has also reported a positive effect of blocking p53-induced apoptosis on normal embryo development (Jin *et al.*, 2009). Importantly, results indicate that while the p53-induced apoptosis pathway is directly accountable for embryo selection during normal preimplantation development, it is neither an impairing factor during oocyte-mediated reprogramming nor a selection determinant for SCNT embryos. However, inhibition of p53 during preimplantation development of young oocyte-derived SCNT embryos led to an increase in outgrowth formation, the first step in ESC derivation. This suggests that p53 plays a direct role in determining the potential of SCNT embryos to give rise to ESCs, possibly by influencing the quality of the trophectoderm. This proposed role of p53 in oocyte-iPS would resemble that found in reprogramming by iPS, which is blocked upon the induction of p53-dependent apoptosis (Marión *et al.*, 2009).

Climacteric oocytes: risk for reproduction and potential for patient-specific ESCs

By using ICSI-derived embryos as experimental control for SCNT, our study further shows that oocytes from climacteric B6C3F1 mice are not only able to sustain *in vitro* fertilization, but even support higher blastocyst rates after sperm injection compared to younger oocytes. Similar to our results, a previous study had shown that *in vitro* matured oocytes from mice in reproductive decay have the capacity for *in vitro* fertilization, and also postimplantation development, albeit at substantially lower rates (Eppig & O'Brien, 1995). Importantly, work in human has shown that successful preimplantation development to blastocyst *in vitro* is possible despite chromosomal abnormalities (Sandalinas *et al.*, 2001), emphasizing the importance of postimplantation stages in embryo selection. A recent report further emphasizes that, despite the absence of detectable changes in acquisition and maintenance of DNA methylation patterns until mid-gestation, there are negative effects of maternal age on mouse postimplantation embryonic and placental development (Lopes *et al.*, 2009). These observations strongly suggest that the factors required for the events following fertilization and preimplantation development are tightly regulated and preserved in the oocyte with aging, but that marks are left which may be detectable as complications only after implantation. In this context, the transfer of fertilized oocytes of older women into younger surrogate mothers continues to bring about health concerns, and consequently social controversy, as that often surrounding current assisted reproductive technologies (Frazzetto, 2004). In a field where investigation using human material is restricted on legal and ethical grounds, the use of the mouse model continues to help elucidating biological mechanisms of aging. In this context, the use of hybrid strains like the one used in this study is proposed to reflect the outbred condition of humans more closely than inbred ones, owing to the larger allelic pool.

Importantly, competence of climacteric mouse oocytes for pluripotency has been demonstrated recently. While a previous study suggested that ESC features might be lost during aging – after the identification of age-induced changes in expression of oocytic stemness genes like DNA methyltransferases and chromatin remodeling factors (Hamatani *et al.*, 2004), Huang and colleagues demonstrated the ability of oocytes from C57Bl/6 mice in reproductive decline to yield pluripotent ESCs after parthenogenetic activation (Huang *et al.*, 2009). Here, we demonstrate that oocytes derived from mice of similar reproductive condition are also able to reprogram somatic nuclei to a pluripotent cell-like state after SCNT, as shown by the derivation of pluripotent ESC lines. In this context, and provided appropriate investigation in humans, we further suggest that eggs from donors in reproductive decline could serve as reliable bioreactors for iPS, for the study of oocyte-induced reprogramming toward patient-specific ESC derivation.

Experimental procedures

Animal handling and oocyte manipulation

Mice were maintained and used for experiments according to the ethical permit issued by the Landesamt für Natur, Umwelt

und Verbraucherschutz (LANUV) of the state of North Rhine-Westphalia, Germany. Throughout the extended time of this study, mice were housed in groups of five in individually ventilated type II-L cages, were exposed to 14L:10D hours photoperiod, and were fed *ad libitum* on Harlan-Teklad 2020SX diet (Harlan Laboratories, Oxford, UK). Oocytes from mice of the B6C3F1 strain (C57Bl/6J × C3H/HeN) were used, as this hybrid strain has been extensively shown to sustain successful reprogramming to pluripotency and totipotency (Wakayama & Yanagimachi, 2001). Mice were either purchased from Harlan Laboratories or bred in-house. Estrous cycle determination was performed by histological evaluation of vaginal smears (15 mice per age group) taken daily over 1 month (prior to sacrifice), as described before (Nelson *et al.*, 1982). Young and aged females were superovulated by injection of 10 international units (IU) of pregnant mare serum gonadotropin (Calbiochem; EMD Biosciences, San Diego, CA, USA), followed by 10 IU of hCG (Calbiochem) 48 h later. A subgroup of animals was weighed (10–26 mice per age group). Animals were sacrificed after cervical dislocation 14 h after hCG injection, and oocytes retrieved from oviduct ampullae. Oocytes and cumulus cells were handled in Hepes-buffered CZB (HCZB) medium, as previously described (Cavaleri *et al.*, 2008). Oocytes were separated from cumulus cells by treatment with 50 IU mL^{-1} hyaluronidase (ICN Biomedicals, Eschwege, Germany) in HCZB, followed by gentle pipetting. Cells were placed in embryo culture medium, consisting of alpha modified Eagle's medium (α-MEM; M4526 Sigma, Seelze bei Hannover, Germany) supplemented with 0.2% w/v BSA (Pentex; Serological Proteins Inc., Kankakee, IL, USA) and 50 μg mL^{-1} gentamicin sulfate (ICN Biomedicals) at 37 °C and under 5% CO_2 until use.

Oocyte micromanipulation and embryo culture

Micromanipulations and embryo culture were performed at 30 °C (room temperature), as previously described (Balbach *et al.*, 2007; Cavaleri *et al.*, 2008). For SCNT, oocytes were first enucleated (spindle-chromosome complex removed) before transfer of one cumulus cell nucleus, with a micropipette driven by a piezo actuator under DIC optics. Cumulus cells used were either from a 5-week-old B6C3F1 oocyte donor or from a 8-week-old mouse expressing an *Oct4* promoter-driven GFP transgene [OG2; B6; CBA-Tg(Pou5f1-EGFP)2Mnn/J, JAX stock number 004654]. The reconstructed oocytes were activated for 6 h in calcium-free embryo culture medium supplemented with 10 mM $SrCl_2$ (ICN) and 5 μg mL^{-1} cytochalasin B (Calbiochem). Intracytoplasmic sperm injection (ICSI) into intact oocytes was used as the fertilization control condition, using sperm from 5-week-old mice of C57Bl/6 or OG2 strains, with manipulation as described before (Balbach *et al.*, 2007; Cavaleri *et al.*, 2008). Embryos were placed in embryo culture medium and cultured at 37 °C under 5% CO_2. For experiments aiming inhibition of the p53-induced apoptosis pathway, SCNT and ICSI were performed using 5-week-old B6C3F1 oocyte donors. Embryos were cultured in embryo culture medium as described previously, in the absence or presence of 1 μM pifithrin-α [2-(2-Imino-4,5,6,7-tetrahydrobenzothiazol-3-yl)-1-p-tolylethanone, HBr; Calbiochem] from the time of activation to the morula stage (72 h). On day 5 after activation, pifithrin-treated and untreated SCNT and ICSI blastocysts were put in culture with γ-ray inactivated mouse embryonic fibroblasts (MEFs), prepared for mouse ESC derivation as described previously (Cavaleri *et al.*, 2008); outgrowth formation was evaluated on day 4 after start of culture on MEFs.

Acquisition and analysis of GFP images

Seventy-eight hours after ICSI or SCNT activation, morulae were imaged for GFP intensity, as previously described (Cavaleri *et al.*, 2008). Embryos were placed individually in 1-μL drops of embryo culture medium on a 50-mm thin-bottom plastic dish (Lumox hydrophilic dish; Greiner Bio-One, Frickenhausen, Germany), overlaid with mineral oil (M8410 Sigma). Live images were captured on stage of an inverted microscope (Eclipse 2000-U; Nikon, Düsseldorf, Germany) coupled to a spinning disk confocal unit (Ultra View RS3; Perkin-Elmer LAS, Jügesheim, Germany). A Nikon CFI Plan Apochromat VC 60X water immersion lens was used to convey 488 nm laser excitation to the embryo (Argon/Krypton laser; Melles Griot, Albuquerque, NM, USA). Five optical sections were captured using a Hamamatsu ORCA ER digital camera (Hamamatsu Photonics KK, Tokyo, Japan). Maximum projections were analyzed with ImageJ (Abramoff *et al.*, 2004). Region of interest (ROI) was drawn with the polygon selection tool, to include only pixels belonging to the embryo. Mean intensity was determined, also for a ROI outside the embryo (taken as background intensity, and thereby subtracted to the intensity measured for the embryo).

ATP and hydrogen peroxide content analysis

ATP levels in oocytes or embryos were determined using an ATP-dependent luciferase–luciferin reaction system. Five to eight oocytes or blastocysts were collected in 200 μL of milli-Q water and vortexed for 1 min. Samples were heated to 95 °C for 20 min to inactivate ATP-degrading enzymes, and then stored until measurement at −80 °C. Samples were incubated in 1 mol L^{-1} $MgCl_2$, 2 mol L^{-1} KCl, and 0.2 mol L^{-1} phosphoenolpyruvate, at 30 °C for 15 min. A luciferase–luciferin mix (ENLITEN; Promega, Mannheim, Germany) was then mixed using an automated system, and light emission detected using a luminometer equipped with a single photon counter (Tecan GENios Pro; Tecan Group Ltd, Männedorf, Switzerland). Levels of ATP were extrapolated from a calibration curve based on known concentrations of ATP (Sigma). Formation of hydrogen peroxide (and related peroxides) was quantified by determining the fluorescence of the probe DCHFDA (2′,7′-dichlorodihydrofluorescein diacetate; Fluka, Sigma). Oocytes or ICSI blastocysts (6–8 per age group) were incubated in embryo culture medium containing 10 μM DCHFDA during 15 min. Cells were briefly washed in culture medium and quickly imaged in individual drops, as

described for acquisition of GFP images. Images were taken at five time points, 10 s apart (200–400 ms exposure, 2 × 2 binning), allowing observation of increase in fluorescence signal because of ROS (induced by laser exposure) and thereby confirming probe-specific signal. Images from the first time point were analyzed, also as described in the previous section. Region of interest was taken for the whole cell for oocytes, and for two different regions of the trophectoderm for blastocysts.

Histological ovary preparation

All chemicals used for histological preparation were from Applichem (Darmstadt, Germany), except when stated otherwise. Ovaries collected from young and aged females were fixed in Bouin's solution (Sigma) and kept at 4 °C until processing. Specimens were embedded in paraffin and sectioned into 10-μm-thick slices, spaced 10 μm apart (total of 10 slices per ovary, four ovaries per age group). Sections were deparaffinized in 100% xylol (two times for 10 min), followed by 1-min long successive washes in an isopropanol gradient (100, 90, and 70%). Eosin staining was performed in 0.1% eosin for 3 min. Sections were washed in an isopropanol gradient (100, 90% for 3 min, and 70% for 10 min) and prepared for histological examination (cover slip fixed with Cytoseal XYL, Microm, Walldorf, Germany). Follicles were scored only when oocytes were visible, for primordial and primary follicles.

Statistical analysis

Fit to logistic regression model (Hothorn *et al.*, 2006), Student's and Welch Two Sample *t*-test, as well as Fisher's test, were performed using R (http://www.r-project.org/). Statistical significance was accepted when $P < 0.05$.

Global transcriptome analysis by microarray

Total mRNA was isolated for samples from young and climacteric mice (pools of 20 ooplasts, and 21–32 SCNT blastocysts in duplicate), using a RNeasy Mini kit (Qiagen, Hilden, Germany), as described by the manufacturer (no DNase treatment). RNA concentrations, as well as purity and integrity check, were determined with Agilent Bioanalyzer 2100 and RNA Pico 6000 Lab-Chip kit (Agilent Technologies). RiboAmp HS Plus Amplification kit (MDS Analytical Technologies, Ismaning, Germany) was used to amplify the total mRNA with two rounds of amplification, according to the manufacturer's instructions. Amplified RNA was eluted with 15 μL of RE Buffer included in the RiboAmp HS Plus Amplification kit. RNA concentrations were determined with Agilent Bioanalyzer 2100 and RNA Pico 6000 Lab-Chip kit. Turbo Labeling CY3 kit (MDS Analytical Technologies) was used to label 3 μg of amplified RNA with Cy3. Concentration and frequency of incorporation were measured with NanoPhotometer (Implen, Munich, Germany). Microarray wash and detection of the labeled RNA on GeneChips were carried out according to the manufacturer's instructions (Agilent Technologies). Gene expression profiling was performed using Agilent Whole Mouse Genome Oligo Microarrays (4 × 44 k, each array containing 41174 features). Array image acquisition and feature extraction were performed using Agilent G2505B Microarray Scanner and FEATURE EXTRACTION software v.9.5 (Agilent Technologies).

Microarray data processing

The microarrays were normalized using the quantile method. The lists of genes differentially expressed between young and climacteric ooplasts, or young and climacteric SCNT blastocysts, were obtained based on the presence of a signal in at least one of the compared samples (flag-filtering), and on at least $\log_2$-fold two difference between normalized expression levels. The GO terms were taken from the AMIGO GO database (Ashburner *et al.*, 2000). The significance (*P*-value) of the GO terms enrichment was assessed using the hypergeometric test. The multitest effect influence was corrected through controlling the false discovery rate using the Benjamini-Hochberg correction at a significance level $\alpha = 0.05$.

Analysis of gene expression by real-time RT–PCR

Real-time analysis of expression of selected genes was performed in the RNA samples for ooplasts and blastocysts, after amplification (same sample as used in microarray detection). Complementary DNA synthesis from 2 μg RNA was performed using a High Capacity cDNA Reverse Transcription kit (Applied Biosystems, Foster City, CA, USA). Transcript levels were determined in triplicate for 20-μL reaction mix per well consisting of cDNA (1:10 dilution), primers, H_2O, and Power SybrGreen PCR Mastermix (Applied Biosystems), using the ABI PRISM Sequence Detection System 7900ht (Applied Biosystems). Primer sequences are given in Table S2 (Supporting Information). Run conditions were as follows: 50 °C for 2 min, 95 °C for 10 min, 95 °C for 10 s, and 60 °C for 1 min for a total of 40 cycles; dissociation step: 95 °C for 15 s, 60 °C for 15 s, and 95 °C for 15 s. Amplification curves and gene expression were normalized to mouse *Gapdh*. Ct-values were obtained with SDS 2.2 (Applied Biosystems), with a threshold of 0.2 and baseline 3–15.

Immunocytochemistry for Oct4 detection in oocytes

Oocytes were retrieved as for all other experiments (described in the previous sections), from 5- and 50-week-old B6C3F1 donors. As Oct4 detection in metaphase II oocytes is difficult, because of lack of nuclear envelope and consequent dilution of the protein in a large cytoplasmic volume, oocytes were parthenogenetically induced to form pronuclei; Oct4 is then expected to be mainly located in the pronuclei, allowing easier visualization after specific immunostaining. For this purpose, cumulus cell-free oocytes were subjected to parthenogenetic stimulus with calcium-free α-MEM containing 10 mM $SrCl_2$ (ICN) and

5 μg mL^{-1} cytochalasin B (Calbiochem). Six hours after activation, the pronuclear stage oocytes were processed for immunostaining as previously described (Cavaleri *et al.*, 2008). In brief, samples were fixed in 1% paraformaldehyde (MP Biomedicals, Illkirch, France), in PBS, for 20 min at room temperature. After fixation, samples were permeabilized with Triton X-100 (0.1% v/v) for 20 min. After permeabilization, samples were incubated at 4 °C in blocking solution containing 2% BSA (w/v), 2% glycine and 5% donkey serum, until further processing. Samples were transferred into 1:2000 dilution of primary antibody (mouse anti-Oct3/4 N-19 goat polyclonal IgG; sc-8628; Santa Cruz, CA, USA) in a 1:4 dilution of blocking solution and incubated overnight. After two washes in PB-T (PBS containing 0.1% Tween 20), specimens were incubated at room temperature in a 1:4 dilution of blocking solution containing secondary rabbit anti-goat antibody coupled to Alexa fluorophore 647 (Molecular Probes - Invitrogen, Darmstadt, Germany), used at a dilution of 1:2000. Samples were washed twice in PBT (phosphate buffer + Tween-20 0.1%) and imaged by spinning disk laser confocal microscopy. Image acquisition and analysis was performed as described in the section relative to the acquisition of GFP images. Oct4-specific fluorescence was determined by analyzing two sections of each activated oocyte, i.e. those containing the largest area of each pronucleus; fluorescence level was determined for both cytoplasm and pronucleus separately.

Derivation of ESCs

Derivation of ESC lines from climacteric SCNT blastocysts was performed as described previously (Cavaleri *et al.*, 2008). After zonae pellucidae removal with Tyrode's solution (Sigma), blastocysts produced by SCNT of OG2 cumulus cells (i.e. containing *Oct4-GFP*) into ooplasts of climacteric donors (47–56 weeks old) were transferred onto a feeder layer of γ-ray-inactivated MEFs (C3H background) previously grown to confluence in four-well dishes. At day 7 after SCNT, blastocysts attached to the feeders forming trophoblastic outgrowths. The inner cell masses (ICMs) were removed with a polished glass pipette, trypsinized with 0.25% trypsin-EDTA (Gibco, Gaithersburg, MD, USA) and reseeded onto fresh feeder cells on a 96-well plate. Passage zero ESCs (after initial plating of the dissociated ICMs) were grown for 6 days in culture and further expanded by subsequent passaging (2–3 days) onto larger well sizes. ESC culture media consisted of Knockout DMEM (Gibco) with 15% serum replacement (Gibco), 5% fetal bovine serum (FBS; BioWest, Nuaillé, France), glutamine and penicillin/streptomycin (Gibco), nonessential amino acids (PAA Laboratories, Pasching, Austria), mercaptoethanol (Gibco), and 2000 Units mL^{-1} leukemia inhibitory factor (produced in-house by overexpression in E. coli, GST-tag purification and tag removal by thrombin).

In vitro differentiation of climacteric SCNT-ESC lines

The ability of the derived climacteric SCNT-ESCs to differentiate *in vitro* was assessed after embryoid body (EB) formation. Embryoid bodies were produced using the hanging drop method (500 ESCs per 20 μl), after feeder cells removal by sedimentation. After 3 days in culture with ESC media, EBs were plated on gelatinized plates for endoderm and mesoderm differentiation, and on matrigel-coated plates for ectoderm differentiation. For mesoderm and endoderm differentiation, EBs were cultured in ESC media modified to contain 15 and 20% FBS instead of serum replacement, respectively, and no leukemia inhibitory factor. For ectoderm differentiation, EBs were cultured in media consisting of a 1:1 mixture of DMEM/F12 (1:1; Gibco) and Neurobasal medium (Gibco), 0.2% BSA fraction V (7.5%; Gibco), 0.5% N2 supplement (Invitrogen, Darmstadt, Germany), 1% B27 supplement (Invitrogen), glutamine/penicillin/streptomycin, mercaptoethanol, and 20 μM activin-like kinase inhibitor SB431542 (Ascent Scientific, Bristol, UK). After 2 weeks of differentiation, cells were fixed in 4% PFA in PBS for 10 min, briefly washed with PBS, and finally with 50 mM glycine in PBS for quenching of residual PFA. The fixed cells were permeabilized with 0.2% Triton X-100 in PBS for 10 min, washed with PBS, and blocked with 2% filtered FBS in PBS-T for 45 min. Primary antibodies for ectoderm (Tuj1 beta-III-tubulin; Sigma T8660, 1:1000), for mesoderm (SMA; Dako M0851, 1:80; Dako, Hamburg, Germany), and for endoderm (Sox17; R&D AF1924, 1:50; R&D, Wiesbaden, Nordenstadt) diluted in blocking solution were applied and incubated overnight at 4 °C. After washing with PBS-T, alexa-fluor-568-coupled secondary antibody (anti-goat A11079 and anti-mouse A11061; Invitrogen) was applied in a 1:500 dilution in PBS/20% blocking solution, incubated for 1 h, and then washed with PBS-T. Hoechst-33342 (Fluka) 5 μg mL^{-1} in PBS was used for nuclei counterstaining, and samples were analyzed for fluorescence.

Teratoma formation by SCNT-ESCs

Single cell–suspended ESCs were injected subcutaneously in the neck region of Scid male mice (1–2 × 10^6 cells per 200 μL) to evaluate the ability to form teratomas. Mice were sacrificed 3 weeks after injection; teratomas were excised, fixed in 4% PFA–PBS for 48 h. Successive washes were performed – once in running water, a gradient of 40%, 70%, 90%, and 100% ethanol, 100% isopropanol and 100% xylol, 30 min each wash – before embedding the teratomas in paraffin, staining with hematoxylin and eosin, and sectioning for histological examination.

Germline contribution of climacteric SCNT-ESCs

Injection of the derived climacteric SCNT-ESCs into fertilized blastocysts and in-utero transfer of the resulting embryos was performed, to determine germline transmission of the cells. In brief, the derived cells were separated from the feeders via double sedimentation, consisting of two times 45-min incubation on plates coated with 0.1% gelatine-PBS. Ten to fifteen ESCs were microinjected into the cavity of 3.5 dpc blastocysts (B6C3 F1

female × CD1 male). The chimeric blastocysts were transferred to the uterus of 3 dpc pseudopregnant CD1 mice 2 h after injection, as previously described (Boiani *et al.*, 2002). Germline contribution was determined after dissection of fetuses at 13.5 dpc and analysis of the gonads (fluorescence imaging for detection of GFP signal).

Acknowledgments

This study was supported by the Deutsche Forschungsgemeinschaft (Special Priority Programme no.1356) and by the Max-Planck Society. The authors are thankful to the Max-Planck Institute for Molecular Biomedicine for logistical support. In the Max-Planck Institute for Molecular Biomedicine, the authors thank Bärbel Schäfer for performing ovarian and teratoma histology, Caroline Schwarzer for preparation of MEF cultures, Davood Sabour for mouse embryo gonad dissection and David Obridge, Ludger Recker and Christin Schmidt for animal maintenance and handling. Thank you also to Dr. Nicole Bäumer and Dr. Sonja Sielker (Arrows Biomedical GmbH, Münster, Germany) for microarray processing and initial data analysis, and to Prof. Torsten Hothorn (LMU Munich, Germany) for useful advice on statistical analysis.

Author contributions

TC Esteves: animal colony management, superovulation, oocyte retrieval, embryo culture, ATP and hydrogen peroxide measurements, histology, characterization of estrous cycle, ESC derivation and culture, immunocytochemistry data analysis, manuscript preparation. ST Balbach: confocal imaging, image analysis, statistical analysis, manuscript preparation. MJ Pfeiffer: superovulation, oocyte retrieval, ESC culture, *in vitro* differentiation, mRNA extraction in single oocytes and *Oct4* mRNA quantification, data analysis, manuscript preparation. MJ Araúzo-Bravo: microarray data processing. DC Klein: superovulation, histology analysis, characterization of estrous cycle. M Sinn: real-time RT–PCR, data analysis. M Boiani: superovulation, oocyte retrieval, SCNT and ICSI micromanipulation, embryo culture, blastocyst injection, teratoma assay, data analysis, manuscript preparation.

References

Abramoff MD, Magelhaes PJ, Ram SJ (2004) Image processing with ImageJ. *Biophotonics Int.* **11**, 36–42.

Ashburner M, Ball CA, Blake JA, Botstein D, Butler H, Cherry JM, Davis AP, Dolinski K, Dwight SS, Eppig JT, Harris MA, Hill DP, Issel-Tarver L, Kasarskis A, Lewis S, Matese JC, Richardson JE, Ringwald M, Rubin GM, Sherlock G (2000) Gene ontology: tool for the unification of biology. The Gene Ontology Consortium. *Nat. Genet.* **25**, 25–29.

Balbach ST, Jauch A, Bohm-Steuer B, Cavaleri FM, Han YM, Boiani M (2007) Chromosome stability differs in cloned mouse embryos and derivative ES cells. *Dev. Biol.* **308**, 309–321.

Banito A, Rashid ST, Acosta JC, Li S, Pereira CF, Geti I, Pinho S, Silva JC, Azuara V, Walsh M, Vallier L, Gil J (2009) Senescence impairs successful reprogramming to pluripotent stem cells. *Genes Dev.* **23**, 2134–2139.

Beetschen JC, Fischer JL (2004) Yves Delage (1854–1920) as a forerunner of modern nuclear transfer experiments. *Int. J. Dev. Biol.* **48**, 607–612.

Boiani M, Eckardt S, Schöler HR, McLaughlin KJ (2002) Oct4 distribution and level in mouse clones: consequences for pluripotency. *Genes Dev.* **16**, 1209–1219.

Boyer LA, Mathur D, Jaenisch R (2006) Molecular control of pluripotency. *Curr. Opin. Genet. Dev.* **16**, 455–462.

Brown KD, Robertson KD (2007) DNMT1 knockout delivers a strong blow to genome stability and cell viability. *Nat. Genet.* **39**, 289–290.

Cavaleri FM, Balbach ST, Gentile L, Jauch A, Bohm-Steuer B, Han YM, Scholer HR, Boiani M (2008) Subsets of cloned mouse embryos and their non-random relationship to development and nuclear reprogramming. *Mech. Dev.* **125**, 153–166.

Eichenlaub-Ritter U (2002) Ageing and aneuploidy in oocytes. *Ernst Schering Res. Found. Workshop* **41**, 111–136.

Eichenlaub-Ritter U, Chandley AC, Gosden RG (1988) The CBA mouse as a model for age-related aneuploidy in man: studies of oocyte maturation, spindle formation and chromosome alignment during meiosis. *Chromosoma* **96**, 220–226.

Eppig JJ, O'Brien M (1995) In vitro maturation and fertilization of oocytes isolated from aged mice: a strategy to rescue valuable genetic resources. *J. Assist. Reprod. Genet.* **12**, 269–273.

Frazzetto G (2004) DNA or loving care? *EMBO Rep.* **5**, 1117–1119.

Gosden RG (1974) Survival of transferred C57BL mouse embryos: effects of age of donor and recipient. *Fertil. Steril.* **25**, 348–351.

Gosden RG, Laing SC, Felicio LS, Nelson JF, Finch CE (1983) Imminent oocyte exhaustion and reduced follicular recruitment mark the transition to acyclicity in aging C57BL/6J mice. *Biol. Reprod.* **28**, 255–260.

Grøndahl ML, Yding Andersen C, Bogstad J, Nielsen FC, Meinertz H, Borup R (2010) Gene expression profiles of single human mature oocytes in relation to age. *Hum. Reprod.* **25**, 957–968.

Hall VJ, Compton D, Stojkovic P, Nesbitt M, Herbert M, Murdoch A, Stojkovic M (2007) Developmental competence of human in vitro aged oocytes as host cells for nuclear transfer. *Hum. Reprod.* **22**, 52–62.

Hamatani T, Falco G, Carter MG, Akutsu H, Stagg CA, Sharov AA, Dudekula DB, VanBuren V, Ko MS (2004) Age-associated alteration of gene expression patterns in mouse oocytes. *Hum. Mol. Genet.* **13**, 2263–2278.

Hiiragi T, Solter D (2005) Reprogramming is essential in nuclear transfer. *Mol. Reprod. Dev.* **70**, 417–421.

Hothorn T, Hornik K, van de Wiel MA, Zeileis A (2006) A Lego system for conditional inference. *Am. Stat.* **60**, 257–263.

Huang J, Okuka M, Wang F, Zuo B, Liang P, Kalmbach K, Liu L, Keefe DL (2009) Generation of pluripotent stem cells from eggs of aging mice. *Aging Cell* **9**, 113–125.

Huangfu D, Maehr R, Guo W, Eijkelenboom A, Snitow M, Chen AE, Melton DA (2008) Induction of pluripotent stem cells by defined factors is greatly improved by small-molecule compounds. *Nat. Biotechnol.* **26**, 795–797.

Igarashi H, Takahashi T, Takahashi E, Tezuka N, Nakahara K, Takahashi K, Kurachi H (2005) Aged mouse oocytes fail to readjust intracellular adenosine triphosphates at fertilization. *Biol. Reprod.* **72**, 1256–1261.

Jin XL, Chandrakanthan V, Morgan HD, O'Neill C (2009) Preimplantation embryo development in the mouse requires the latency of TRP53 expression, which is induced by a ligand-activated PI3 kinase/AKT/MDM2-mediated signaling pathway. *Biol. Reprod.* **81**, 234–242.

Johnson FB, Sinclair DA, Guarente L (1999) Molecular biology of aging. *Cell* **96**, 291–302.

Jones EC, Krohn PL (1961) The relationships between age, numbers of oocytes and fertility in virgin and multiparous mice. *J. Endocrinol.* **21**, 469–495.

Jurisicova A, Varmuza S, Casper RF (1996) Programmed cell death and human embryo fragmentation. *Mol. Hum. Reprod.* **2**, 93–98.

Kawamura T, Suzuki J, Wang YV, Menendez S, Morera LB, Raya A, Wahl GM, Belmonte JC (2009) Linking the p53 tumour suppressor pathway to somatic cell reprogramming. *Nature* **460**, 1140–1144.

Kim J, Chu J, Shen X, Wang J, Orkin SH (2008) An extended transcriptional network for pluripotency of embryonic stem cells. *Cell* **132**, 1049–1061.

Kishigami S, Mizutani E, Ohta H, Hikichi T, Thuan NV, Wakayama S, Bui HT, Wakayama T (2006) Significant improvement of mouse cloning technique by treatment with trichostatin A after somatic nuclear transfer. *Biochem. Biophys. Res. Commun.* **340**, 183–189.

Kujjo LL, Laine T, Pereira RJ, Kagawa W, Kurumizaka H, Yokoyama S, Perez GI (2010) Enhancing survival of mouse oocytes following chemotherapy or aging by targeting Bax and Rad51. *PLoS ONE* **5**, e9204.

Li HJ, Liu DJ, Cang M, Wang LM, Jin MZ, Ma YZ, Shorgan B (2009) Early apoptosis is associated with improved developmental potential in bovine oocytes. *Anim. Reprod. Sci.* **114**, 89–98.

Liu G, Kato Y, Tsunoda Y (2007) Aging of recipient oocytes reduces the development of cloned embryos receiving cumulus cells. *J. Reprod. Dev.* **53**, 785–790.

Lopes FL, Fortier AL, Darricarrere N, Chan D, Arnold DR, Trasler JM (2009) Reproductive and epigenetic outcomes associated with aging mouse oocytes. *Hum. Mol. Genet.* **18**, 2032–2044.

Marión RM, Strati K, Li H, Murga M, Blanco R, Ortega S, Fernandez-Capetillo O, Serrano M, Blasco MA (2009) A p53-mediated DNA damage response limits reprogramming to ensure iPS cell genomic integrity. *Nature* **460**, 1149–1153.

Miao YL, Kikuchi K, Sun QY, Schatten H (2009) Oocyte aging: cellular and molecular changes, developmental potential and reversal possibility. *Hum. Reprod. Update* **15**, 573–585.

Myers DD (1978) Review of disease patterns and life span in aging mice: genetic and environmental interactions. *Birth Defects Orig. Artic. Ser.* **14**, 41–53.

Nelson JF, Felicio LS, Randall PK, Sims C, Finch CE (1982) A longitudinal study of estrous cyclicity in aging C57BL/6J mice: I. Cycle frequency, length and vaginal cytology. *Biol. Reprod.* **27**, 327–339.

Ono T, Li C, Mizutani E, Terashita Y, Yamagata K, Wakayama T (2010) Inhibition of class IIb histone deacetylase significantly improves cloning efficiency in mice. *Biol. Reprod.* doi: 10.1095/biolreprod.110.085282.

Palmieri SL, Peter W, Hess H, Schöler HR (1994) Oct-4 transcription factor is differentially expressed in the mouse embryo during establishment of the first two extraembryonic cell lineages involved in implantation. *Dev. Biol.* **166**, 259–267.

Pan H, Ma P, Zhu W, Schultz RM (2008) Age-associated increase in aneuploidy and changes in gene expression in mouse eggs. *Dev. Biol.* **316**, 397–407.

Pellestor F, Anahory T, Andréo B, Hédon B, Hamamah S (2004) Maternal aging and aneuploidy: lessons from human oocytes. *Fertil. Steril.* **82**, S281–S282.

Perez GI, Jurisicova A, Wise L, Lipina T, Kanisek M, Bechard A, Takai Y, Hunt P, Roder J, Grynpas M, Tilly JL (2007) Absence of the proapoptotic Bax protein extends fertility and alleviates age-related health complications in female mice. *Proc. Natl. Acad. Sci. U. S. A.* **104**, 5229–5234.

Peters H, Byskov AG, Himelstein-Braw R, Faber M (1975) Follicular growth: the basic event in the mouse and human ovary. *J. Reprod. Fertil.* **45**, 559–566.

Sandalinas M, Sadowy S, Alikani M, Calderon G, Cohen J, Munné S (2001) Developmental ability of chromosomally abnormal human embryos to develop to the blastocyst stage. *Hum. Reprod.* **16**, 1954–1958.

Sauer MV (1998) The impact of age on reproductive potential: lessons learned from oocyte donation. *Maturitas* **30**, 221–225.

Shi W, Zakhartchenko V, Wolf E (2003) Epigenetic reprogramming in mammalian nuclear transfer. *Differentiation* **71**, 91–113.

Shi Y, Desponts C, Do JT, Hahm HS, Scholer HR, Ding S (2008) Induction of pluripotent stem cells from mouse embryonic fibroblasts by Oct4 and Klf4 with small-molecule compounds. *Cell Stem Cell* **3**, 568–574.

Storer JB (1966) Nonspecific life shortening in male mice exposed to the mammary tumor agent. *J. Natl Cancer Inst.* **37**, 211–215.

Surani MA (2001) Reprogramming of genome function through epigenetic inheritance. *Nature* **414**, 122–128.

Taniguchi T, Taniguchi R, Kanagawa H (1996) Influence of oocyte aging on developmental ability of reconstituted embryos produced from oocyte cytoplast and single blastomeres of two-cell stage embryos. *J. Vet. Med. Sci.* **58**, 635–640.

Tarín JJ (1996) Potential effects of age-associated oxidative stress on mammalian oocytes/embryos. *Mol. Hum. Reprod.* **2**, 717–724.

Tarín JJ, Perez-Albala S, Cano A (2000) Consequences on offspring of abnormal function in ageing gametes. *Hum. Reprod Update* **6**, 532–549.

Vassena R, Han Z, Gao S, Latham KE (2007) Deficiency in recapitulation of stage-specific embryonic gene transcription in two-cell stage cloned mouse embryos. *Mol. Reprod. Dev.* **74**, 1548–1556.

Wakayama T, Yanagimachi R (2001) Mouse cloning with nucleus donor cells of different age and type. *Mol. Reprod. Dev.* **58**, 376–383.

Wakayama S, Suetsugu R, Thuan NV, Ohta H, Kishigami S, Wakayama T (2007) Establishment of mouse embryonic stem cell lines from somatic cell nuclei by nuclear transfer into aged, fertilization-failure mouse oocytes. *Curr. Biol.* **17**, R120–R121.

Wang Q, Sun QY (2007) Evaluation of oocyte quality: morphological, cellular and molecular predictors. *Reprod. Fertil. Dev.* **19**, 1–12.

Woodruff RC, Thompson JN Jr (2003) The role of somatic and germline mutations in aging and a mutation interaction model of aging. *J. Anti. Aging Med.* **6**, 29–39.

Yu BP, Chung HY (2006) Adaptive mechanisms to oxidative stress during aging. *Mech. Ageing Dev.* **127**, 436–443.

Supporting Information

Additional supporting information may be found in the online version of this article:

Fig. S1 Correlation between microarray data from Hamatani *et al.* (2004) and the present study.

Fig. S2 Correlation between RT-PCR and microarray data for young and climacteric ooplasts.

Fig. S3 Hierarchical clustering of microarray samples.

Fig. S4 *In vitro* differentiation of climacteric SCNT-ESCs.

Table S1 Significant gene ontology (GO) enrichment terms for differentially expressed genes in SCNT blastocysts derived from young and climacteric ooplasts.

Table S2 Primer sequences for real time PCR (SYBR green).

As a service to our authors and readers, this journal provides supporting information supplied by the authors. Such materials are peer-reviewed and may be re-organized for online delivery, but are not copy-edited or typeset. Technical support issues arising from supporting information (other than missing files) should be addressed to the authors.